

Exergy Analysis of a Double-Stage Organic Rankine Cycle Using Renewable Energy

Ahmet KAPLAN^{*1} ORCID 0000-0002-4094-3180
Arif ÖZBEK² ORCID 0000-0003-1287-9078

¹Mechanical Engineering Department, Engineering Faculty, Cukurova University, Adana

²Mechanical Engineering Department, Ceyhan Engineering Faculty, Cukurova University, Adana

Geliş tarihi: 03.01.2022

Kabul tarihi: 21.03.2022

Atf şekli/ How to cite: KAPLAN, A., ÖZBEK, A., (2022). Exergy Analysis of a Double-Stage Organic Rankine Cycle Using Renewable Energy. Çukurova Üniversitesi, Mühendislik Fakültesi Dergisi, 37(1), 43-54.

Abstract

In this study, exergy analysis of a double-stage Organic Rankine Cycle (ORC) was performed using the Engineering Equation Solver program (EES). For certain temperature limits in the first and second stages (S-I and S-II) R245fa + R245fa was used as refrigerant pair. This study aims to determine the effect of working temperature on system efficiency, exergy efficiency and the most suitable working temperature. The results showed that at 425K, 14.11kW exergy destruction is obtained in Pump-1 higher than other components. The smallest exergy destruction is 0.133kW is observed in Turbine-2 at 400K temperature. The highest thermal and exergy efficiencies of the whole system were obtained at 400K temperature as 8.85% and 48.55%, respectively.

Keywords: Organic Rankine cycle, Exergy analysis, Double stage cycle, Solar power

Yenilenebilir Enerji Kullanan İki Aşamalı Bir Organik Rankine Çevriminin Ekserji Analizi

Özet

Bu çalışmada, Mühendislik Denklem Çözücü programı (EES) kullanılarak çift aşamalı bir Organik Rankine Çevriminin (ORC) ekserji analizi yapılmıştır. Birinci ve ikinci kademelerde (S-I ve S-II) belirli sıcaklık limitleri için R245fa + R245fa akışkan çifti olarak kullanılmıştır. Bu çalışma, çalışma sıcaklığının sistem verimliliğine, ekserji verimliliğine etkisini belirlemeyi ve en uygun çalışma sıcaklığını bulmayı amaçlamaktadır. Sonuçlar, 425K'da Pompa-1'de diğer bileşenlerden daha yüksek 14.11kW ekserji tahribatının elde edildiğini göstermiştir. En küçük ekserji tahribatı 0.133kW olup, Türbin-2'de 400K sıcaklıkta gözlenmektedir. Tüm sistemin en yüksek termal ve ekserji verimleri sırasıyla %8,85 ve %48,55 ile 400K sıcaklıkta elde edilmiştir.

Anahtar Kelimeler: Organik Rankine çevrimi, Ekserji analizi, İki aşamalı çevrim, Güneş enerjisi

*Corresponding author (Sorumlu yazar): Ahmet KAPLAN, ahmttkplnn@gmail.com

1. INTRODUCTION

Energy efficiency is becoming a major concern of 21st century with increasing fossil fuel consumption [1]. The organic Rankine cycle (ORC) is established for converting heat to electricity. Capability of utilization of various kinds of low-grade heat sources for power generation is the most important feature of an ORC [2]. With respect to heat recovery, ORC is an important way to recover low-medium grade heat, but relatively low thermal efficiency is the biggest problem [3]. Wang et al. (2012) have proposed a double stage Organic Rankine Cycle for discontinuous waste heat recovery [4]. Some other heat sources for ORC applications to produce electricity is Biomass, solar thermal energy and geothermal [5]. Wang et al., (2020) explained that numerous researchers have extensively studied the organic Rankine Cycle, focusing mainly on system structure, working fluid, and optimization of cycle parameters [6]. Bertrand et al., (2009) indicated that the refrigerants studied found that the organic rankine cycle's most suitable working fluid for small-scale solar applications was R134a [7].

The term exergy was first used by Carnot in 1824 [8]. Studies on exergy analysis started with Gouy and Stodola. At the beginning of this century, scientists such as Jouguet, Lewiss and Randall, DeBaufre, Darrieus, Keenan, Lerberghe and Glansdorf made great contributions to the development of thermodynamics and the concept of exergy; In 1935, Bosnjakovic started to apply the concept of exergy to the thermodynamic analysis of systems [9]. Exergy is defined as the maximum work that can be obtained from a system by bringing it under the same conditions as the environment [10]. Tantekin et al. (2015) worked on a ORC which is working with R245fa organic refrigerant [11].

When a system is dead state, it is at the same temperature and pressure as its surroundings. In other words, it is in thermal and mechanical or

thermodynamic equilibrium with the environment. Also, the kinetic and potential energies of the system with respect to its surroundings are zero. When the system is dead state, it cannot enter into a chemical reaction with its environment. The dead state properties of the system are P_0 , T_0 , h_0 , u_0 and s_0 . At dead state $P_0=1$ atm (101.325 kPa) and $T_0=25$ °C (298.15 K) [12]. The work potential of the systems will be characterized by exergy analysis. It provides a more realistic view of various devices and processes [13].

In this study, Using the Engineering Equation Solver program (EES) which is the key feature of EES is its highly accurate thermodynamic and transport property database for hundreds of substances, allowing it to be used with equation-solving capability. Using the EES program exergy analysis of a double-stage Organic Rankine Cycle (ORC) was performed. In the first and second stages (S-I and S-II), R245fa organic fluids were used for certain temperature limits. In order to obtain exergy efficiency and exergy destruction rate from ORC.

2. MATERIAL AND METHOD

2.1. System Description

The double stage ORC system designed is shown in Figure 1. The solar collector is used as a heater in this system. Heat is taken from the solar collector and delivered that heat to the working fluid on the first stage at the evaporator. The second-stage working fluid in Re-evaporator is heated with the turbine-1 exit fluid which is still in the superheated gas state. As a pre-heater the regenerator heats the compressed liquid. At both condensers, the water is used as a cooler. The same refrigerant is used in the first stage (S-I) and the second stage (S-II) as working fluid. At the evaporator, Re-evaporator and heat exchangers the effectiveness-NTU method is used to model.

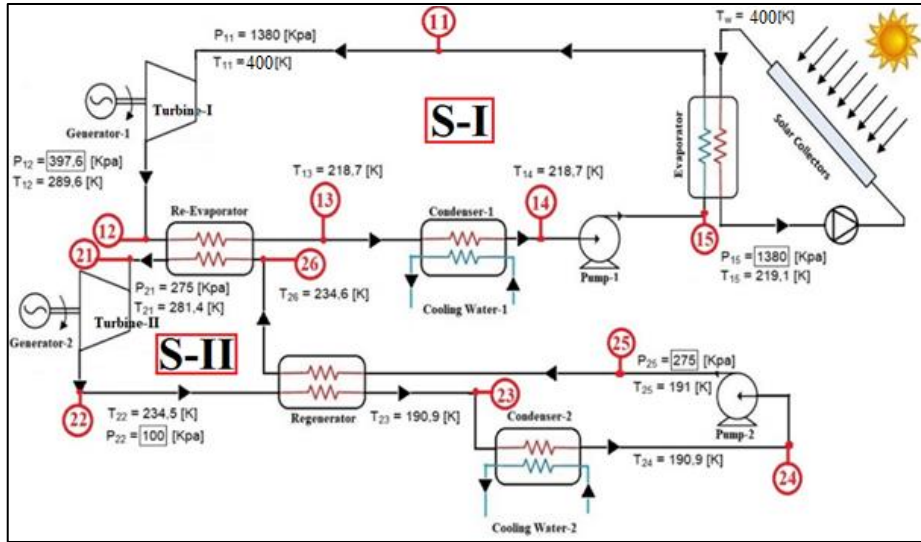


Figure 1. Schematic representation of double stage ORC system

The ORC system consists of two stages. The same fluid is used in the first and second stages (S-I and S-II), and the solar collector gives to the heat in the system. That heat is converted into electric energy. All of the heat sources like natural gas, waste heat, geothermal energy, solar energy etc. can be used instead of solar collector. The system works with 0.93 kg/s and 0.4882 kg/s constant mass flow rate in the first (S-I) and second (S-II) stages, respectively. Also, all components works with constant pressure. Calculations were made between 400K and 425K temperature at which two stage can work.

Figure 2 illustrates the temperature/entropy diagram of the two-stage Rankine cycle designed with R245fa at each stage. The points in the first stage show: 11-12 is the turbine1, 12-13 is the re-evaporator, 13-14 is a condenser1, 14-15 is a pump1, and 15-11 is the evaporator where heat is gained from the solar collector. The points in the second stage show: 21-22 is a turbine2, 22-23 and 25-26 are regenerator, 23-24 is a condenser2, 24-25 is a pump2, and 26-21 is an evaporator where heat is gained from re-evaporator.

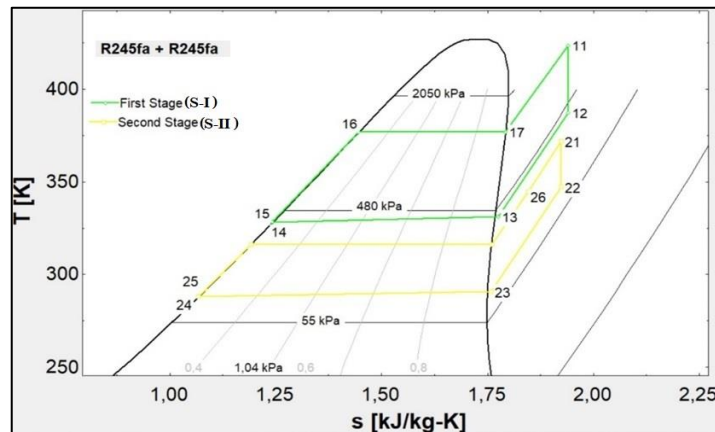


Figure 2. Temperature/entropy chart of two-stage Rankine cycle with R245fa at each stage

2.2. Organic Refrigerants

Efficient working fluid should have a low liquid specific volume and low steam [14]. The specific volume of the fluid pressure in the condenser

should be as small as possible to minimize the feed pump work [15]. Physical, safety and environmental data of the working fluid used in the analyses are shown in Table 1.

Table 1. Physical, safety and environmental data of the working fluid

Substance	Molecular mass (kg/kmol)	T _{bp} (°C)	T _{cr} (°C)	P _{cr} (MPa)	ASHRAE 34 safety group	Atmospheric life time (yr)	ODP	GWP (100 yr)
R245fa	134.05	15.3	154.1	3.64	B1	8.8	0	820

T_{bp}: Normal boiling point; T_{cr}: Critical temperature; P_{cr}: Critical pressure; ODP: Ozone depletion potential, relative to R-11; GWP: Global warming potential, relative to CO₂. n.a: non available.

2.3. Energy Analysis of the System

Because Rankine cycles with four components (pump, boiler, turbine and condenser) accepted as constant-flow devices, all arithmetic operations constituting the Rankine cycle can be analyzed as the fixed-flow process. Potential and kinetic energy are often neglected because they are small in terms of according to work and heat transfer [16].

Pump and turbine are isentropic. Do not require any work at the boiler and condenser. Energy relationship for each device can be expressed as:

S-I Processes: Process 11 - 12 is the Turbine-1 (Equation 1).

$$\dot{W}_{T-I} = \dot{m}_I \times (h_{11} - h_{12}) \times \eta_m \quad (1)$$

At the designed condition the isentropic efficiency of Turbine-1 is $\eta_{T-I} = 0.8$.

Process 12 – 13 is Re-evaporator (Equation 2).

$$\dot{Q}_r = \dot{m}_I \times (h_{12} - h_{13}) \quad (2)$$

Process 13 – 14 is the condenser1 (Equation 3).

$$\dot{Q}_{out-I} = \dot{m}_I \times (h_{13} - h_{14}) \quad (3)$$

Process 14 – 15 is the pump1 (Equation 4).

$$\dot{W}_{p-I} = \dot{m}_I \times (h_{14} - h_{15}) \times \eta_p \quad (4)$$

At the designed condition the pump1 efficiency is $\eta_{p-I} = 0.8$

Process 15 – 11 is a solar collector gives the heat to the system (Equation 5).

$$\dot{Q}_{in} = \dot{m}_I \times (h_{11} - h_{15}) \quad (5)$$

S-II Processes: Process 21 - 22 is the Turbine-2 (Equation 6).

$$\dot{W}_{T-II} = \dot{m}_{II} \times (h_{21} - h_{22}) \times \eta_{T-II} \quad (6)$$

At the designed condition the isentropic efficiency of Turbine-2 is $\eta_{T-2} = 0.8$.

Process 22 – 23 is the Regenerator (Equation 7).

$$\dot{Q}_{R-2} = \dot{m}_{II} \times (h_{22} - h_{23}) \quad (7)$$

The ORC with a regenerator is better than the basic ORC because of when the heat source temperature is relatively high [16].

Process 23 – 24 is the condenser 2 (Equation 8).

$$\dot{Q}_{out-2} = \dot{m}_{II} \times (h_{23} - h_{24}) \quad (8)$$

Process 24 – 25 is the pump 2 (Equation 9).

$$\dot{W}_{p-II} = \dot{m}_{II} \times (h_{24} - h_{25}) \times \eta_{p-II} \quad (9)$$

At the designed condition the pump efficiency is $\eta_{p-II} = 0.8$

Process 25-21 is the Re-evaporator (Equation 10).

$$\dot{Q}_{in-II} = \dot{m}_{II} \times (h_{21} - h_{25}) \quad (10) \quad \dot{Q}_{max} = C_{min} (T_{h-in} - T_{c-in}) \quad (15)$$

The net electrical power produced by the system is calculated from equation below (Equation 11):

$$\dot{W}_{net} = (\dot{W}_{T-I} + \dot{W}_{T-II}) - (\dot{W}_{p-I} + \dot{W}_{p-II}) \quad (11) \quad NTU = \frac{U \times A}{C_{min}} \quad (16)$$

The thermal efficiency of the double stage ORC system is determined as (Equation 12):

$$\eta_{th} = \frac{\dot{W}_{net}}{\dot{Q}_{in}} \quad (12)$$

The effectiveness – NTU Method: Kays and London in 1955 was found The effectiveness-NTU method. Heat exchanger analysis greatly simplified this method [17]. By the ϵ -NTU all heat exchangers are calculated (Equation 13):

$$\epsilon = \frac{\dot{Q}_{act}}{\dot{Q}_{max}} \quad (13)$$

A dimensionless parameter ϵ is the heat transfer effectiveness. Defined with; the ratio of actual heat transfer rate to maximum possible heat transfer rate.

In a heat exchanger to determine the maximum possible heat transfer rate, difference between the inlet temperature of the hot and cold fluids is maximum temperature difference in a heat exchanger [16] (Equation 14).

$$\dot{Q}_{act} = C_h (T_{h-in} - T_{h-out}) = C_c (T_{c-out} - T_{c-in}) \quad (14)$$

The heat capacity of the hot and cold fluids C_h and C_c , respectively (Equation 15).

The smaller fluid thermal capacity is C_{min} . The overall heat transfer coefficient is U (Equation 16).

NTU is a dimensionless number which means number of transfer unit.

2.4. Exergy Analysis

For process components the following exhibits the numerous rate balance values based on energy and exergy approaches. The equations for a steady-state system are given below [18] (Equation 17-19).

$$\sum \dot{m}_i = \sum \dot{m}_e \quad (17)$$

$$Q - W = \sum E_e - \sum E_i \quad (18)$$

$$X - W = \sum X_e - \sum X_i + X_D \quad (19)$$

The general exergy balance is expressed in the rate form as (Equation 20):

$$\dot{E}x_i - \dot{E}x_e = \dot{E}x_D \quad (20)$$

And the specific exergy is calculated as (Equation 21):

$$ex = h - h_0 - T_0(s - s_0) \quad (21)$$

Table 2. Exergy analysis equations for the system components

Stage	Components	Exergy destruction rate	Exergy efficiency
S-I	Turbine-1	$X_D = X_{11} - W_{T1} - X_{12}$	$\eta_{t1} = \frac{W_{T1}}{X_{11} - X_{12}}$
	Condenser-1	$X_D = X_{13} + X_{cw1-in} - X_{14} - X_{cw1-out}$	$\eta_{c1} = \frac{X_{cw1-in} - X_{cw1-out}}{X_{13} - X_{14}}$
	Pump-1	$X_D = X_{14} + W_{P1} - X_{15}$	$\eta_{p1} = \frac{X_{15} - X_{14}}{W_{P1}}$
	Evaporator	$X_D = X_{15} + X_{SC-in} - X_{11} - X_{SC-out}$	$\eta_{evap} = \frac{X_{11} - X_{15}}{X_{SC-in} - X_{SC-out}}$

Table 2. Continou

S-I & S-II	Re-Evaporator	$X_D = X_{12} + X_{26} - X_{13} - X_{21}$	$n_{R-e} = \frac{X_{12} - X_{13}}{X_{26} - X_{11}}$
S-II	Turbine-2	$X_D = X_{21} - W_{T2} - X_{22}$	$n_{t2} = \frac{W_{T2}}{X_{21} - X_{22}}$
	Condenser-2	$X_D = X_{23} + X_{cw2-in} - X_{24} - X_{cw2-out}$	$n_{c2} = \frac{X_{cw2-in} - X_{cw2-out}}{X_{23} - X_{24}}$
	Pump-2	$X_D = X_{24} + W_{P2} - X_{25}$	$n_{p2} = \frac{X_{25} - X_{24}}{W_{P2}}$
	Regenerator	$X_D = X_{22} + X_{25} - X_{23} - X_{26}$	$n_{Rg} = \frac{X_{22} - X_{23}}{X_{25} - X_{26}}$

3. RESULT AND DISCUSSIONS

With the EES (Engineering Equation Solver) software program, thermodynamic properties of the R245fa refrigerant in the first and second stages were determined. EES simplifies the process. EES groups equations and automatically identifies that need to be solved and instead of assignments normally used in formal programming

languages uses equations [15]. The effect on the system in the same situation is calculated by changing the evaporator inlet temperature (T_w).

For Evaporator Inlet Temperature is 400K: Table 3 shows the thermodynamic values of the first stage using R245fa fluid when the evaporator inlet temperature (T_w) is 400K.

Table 3. Thermodynamic properties of R245fa in the first stage

Point	State	Temperature (K)	Pressure (kPa)	Enthalpy (kJ/kg)	Entropy (kJ-kg/K)
11	Superheated vapor	418.5	1380	529.0	1.925
12	Superheated vapor (Scroll expander)	382	397.6	501.2	1.925
13	Superheated vapor	331.3	397.6	447.9	1.776
14	Saturated liquid	328	397.6	273.1	1.243
15	Sub-cooled liquid (Pump)	328.5	1380	273.9	1.243
16	Saturated liquid	377	1380	345.8	1.447
17	Saturated vapor	377	1380	476.3	1.793

Table 4 shows the thermodynamic values of the second stage using R245fa fluid when the evaporator inlet temperature (T_w) is 400K.

Table 4. Thermodynamic properties of R245fa in the second stage

Point	State	Temperature (K)	Pressure (kPa)	Enthalpy (kJ/kg)	Entropy (kJ-kg/K)
21	Superheated vapor	366.8	275	487.3	1.910
22	Superheated vapor (Scroll expander)	342.0	100	465.8	1.910
23	Superheated vapor	290.9	100	418.0	1.759
24	Saturated liquid	288.0	100	219.1	1.068
25	Sub-cooled liquid (Pump)	288.1	275	225.2	1.068
26	Saturated liquid	339.2	275	459.3	1.831
27	Saturated vapor	316.1	275	256.6	1.192

Table 5 shows the power output, thermal efficiency and exergy efficiency values of different evaporator inlet temperature (T_w) for R245fa refrigerant at both stages. According to

the results, the highest power output, thermal efficiency and exergy efficiency values were obtained as 18.99 kW, 8.856% and 48.55%, respectively at 400K.

Table 5. System performance for different temperature for R245fa refrigerant

Turbine Inlet Temperature (K)	Power output (kW)	Thermal Efficiency (%)	Exergy Efficiency System (%)
400	18.99	8.856	48.55
405	18.22	8.274	44.06
410	17.73	7.846	40.63
415	17.40	7.513	37.87
420	17.19	7.246	35.59
425	17.06	7.025	33.66

For Evaporator Inlet Temperature is 425K:
Table 6 and 7 show the thermodynamic values of the first stage and second stage using R245fa

fluid when the evaporator inlet temperature (T_w) is 425K, respectively.

Table 6. Thermodynamic properties of R245fa in the first stage

Point	State	Temperature (K)	Pressure (kPa)	Enthalpy (kJ/kg)	Entropy (kJ-kg/K)
11	Superheated vapor	423.5	1380	535.1	1.940
12	Superheated vapor (Scroll expander)	387.2	397.6	506.7	1.940
13	Superheated vapor	331.3	397.6	447.9	1.776
14	Saturated liquid	328	397.6	273.1	1.243
15	Sub-cooled liquid (Pump)	328.5	1380	273.9	1.243
16	Saturated liquid	377	1380	345.8	1.447
17	Saturated vapor	377	1380	476.3	1.793

Table 7. Thermodynamic properties of R245fa in the second stage

Point	State	Temperature (K)	Pressure (kPa)	Enthalpy (kJ/kg)	Entropy (kJ-kg/K)
21	Superheated vapor	372	275	492.6	1.924
22	Superheated vapor (Scroll expander)	347.2	100	470.8	1.924
23	Superheated vapor	290.9	100	418.0	1.759
24	Saturated liquid	288	100	219.1	1.068
25	Sub-cooled liquid (Pump)	288.1	275	224.8	1.068
26	Saturated liquid	344.4	275	464.5	1.846
27	Saturated vapor	316.1	275	256.6	1.192

Figure 3 shows thermal efficiency and power output relation between 400K and 425K evaporator inlet temperatures. As can be seen from the figure, there is an inverse proportion between thermal efficiency and power output

with evaporator inlet temperature. For the system, both net electrical power and thermal efficiency decrease as ORC working temperature increases.

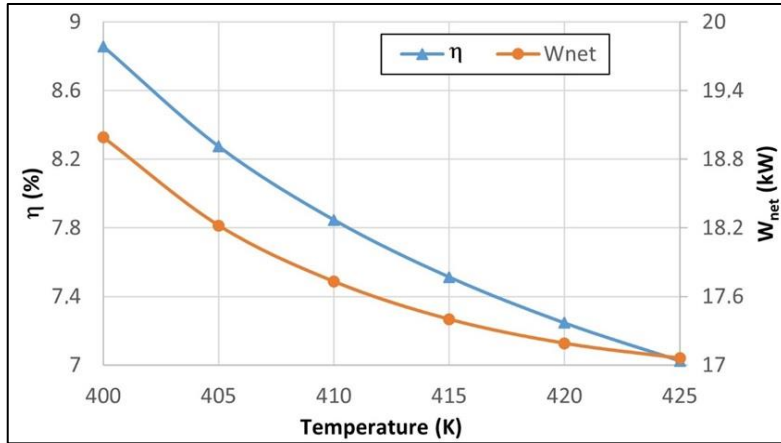


Figure 3. Thermal efficiency and power output values of the system versus evaporator inlet temperatures

The variation of the thermal and exergy efficiencies against the evaporator inlet temperature, for ORC system are shown in Figure 4. It is seen from the figure that, the exergy efficiency of the cycle decreases with increasing

evaporator inlet temperature. At same time, thermal efficiency of the system decreases with increasing evaporator inlet temperature. The highest thermal and exergy efficiencies are seen at the 400K temperature.

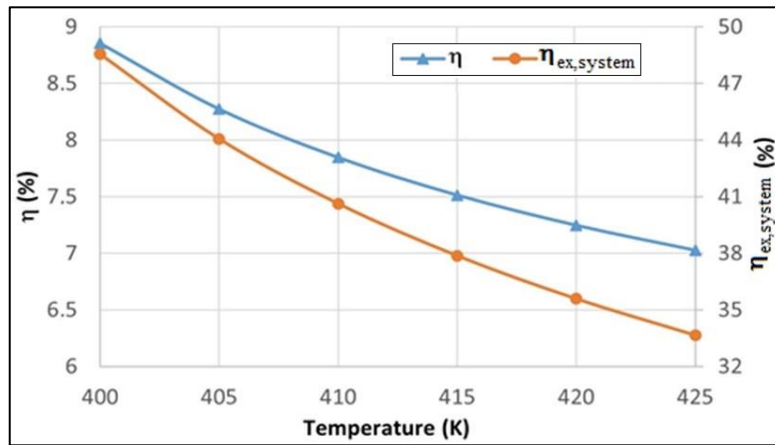


Figure 4. Thermal efficiency and exergy efficiency against evaporator inlet temperatures for the system

Figure 5 represents exergy efficiency and exergy destruction values versus evaporator inlet temperature for Turbine1 and 2. It is seen from the figure that, exergy efficiency in the Turbine-1 decreases, while exergy destruction in the Turbine-1 increases with increasing evaporator inlet temperature. The smallest and highest exergy destructions in the Turbine-1 is 0.4514 kW and 0.6653 kW, respectively. The percentage of the exergy efficiency in Turbine-1 is 98.14 and 97.54

for 400K and 425K, respectively. Figure 5 also shows that, exergy efficiency in the Turbine-2 decreases, while exergy destruction in the turbine-2 increases, when evaporator inlet temperature is increased. The smallest and highest exergy destruction in the Turbine-2 is 0.1258 kW and 0.1496 kW, respectively. The percentage of the exergy efficiency in Turbine-2 is 99.25 and 98.48 for 400K and 425K, respectively.

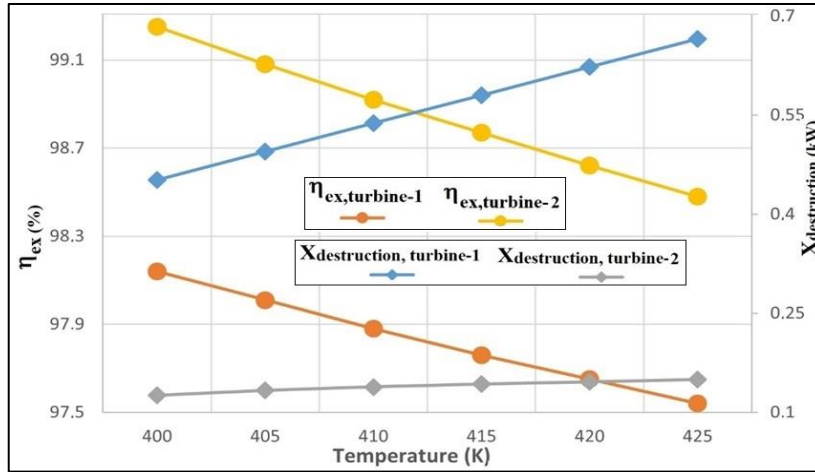


Figure 5. Exergy efficiency and exergy destruction values versus evaporator inlet temperature for Turbine1 and 2

According to Figure 6 a and Figure 7 b, the exergy efficiency reduces with increasing evaporator inlet temperature of hot fluid for Pump1 and 2. In addition, the highest exergy efficiency is calculated as to be 6.18% and 83% for Pump-1 and 2, respectively when the evaporator inlet temperature is 400K. Exergy efficiency values decrease up to 5.48% and 44% for Pump1 and 2.

The exergy destruction is increased from 11.2% to 12.6% for Pump1 and from 1.6% to 3.1% for Pump2 in figure 6 a and b. According to the results of calculations, it is seen from Figure 6 a and Figure 7 b; the highest exergy destruction is observed at the Turbine1 and 2 against to the smallest exergy efficiency is seen at the Condenser1 and 2 for 425K temperature.

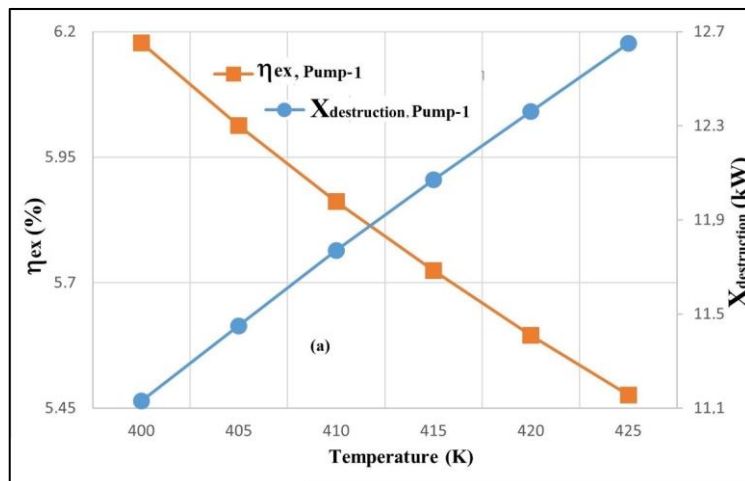


Figure 6. Exergy destruction and Thermal efficiency values when using R245fa at different evaporator inlet temperatures for (a) Pump1

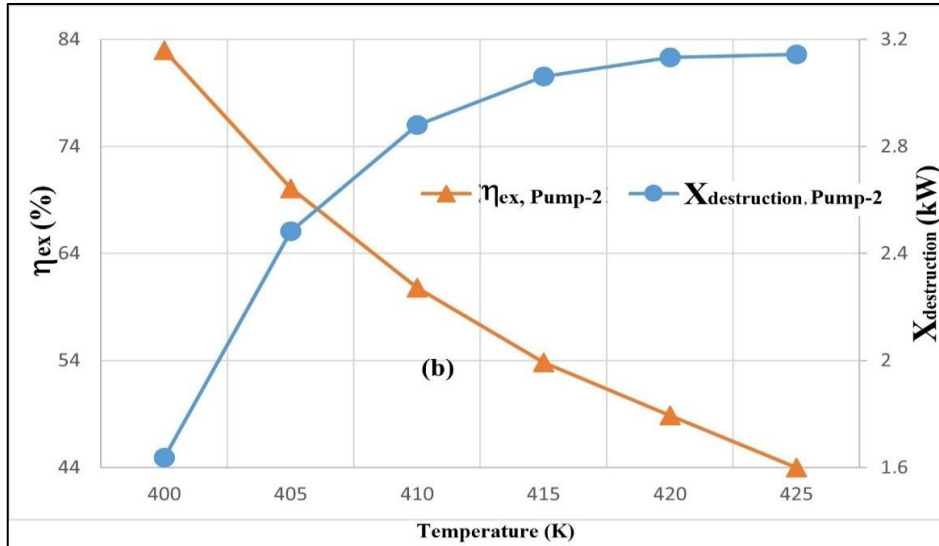


Figure 7. Exergy destruction and Thermal efficiency values when using R245fa at different evaporator inlet temperatures for (b) Pump2

Exergy efficiency values of ORC system components at 425K evaporator inlet temperature are shown in Figure 8. The greatest efficiencies

were obtained in Turbine1 and 2 and in the Evaporator. Smallest efficiencies are obtained in both Condensers and in Pump1.

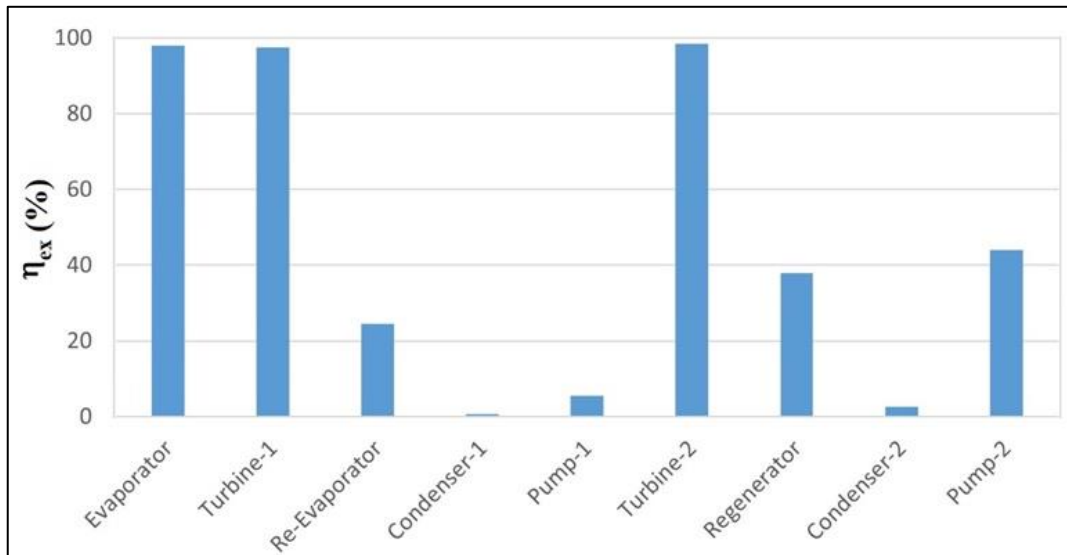


Figure 8. Exergy efficiency values of all components of the system at 425K evaporator inlet temperature

Exergy destruction of the turbines and pumps due to evaporator inlet temperature changes is given in Figure 9. The maximum exergy destruction is found in Pump1 compared to other components for

all temperatures. Minimum exergy destruction is found in Turbine2 compared to other components for all temperatures.

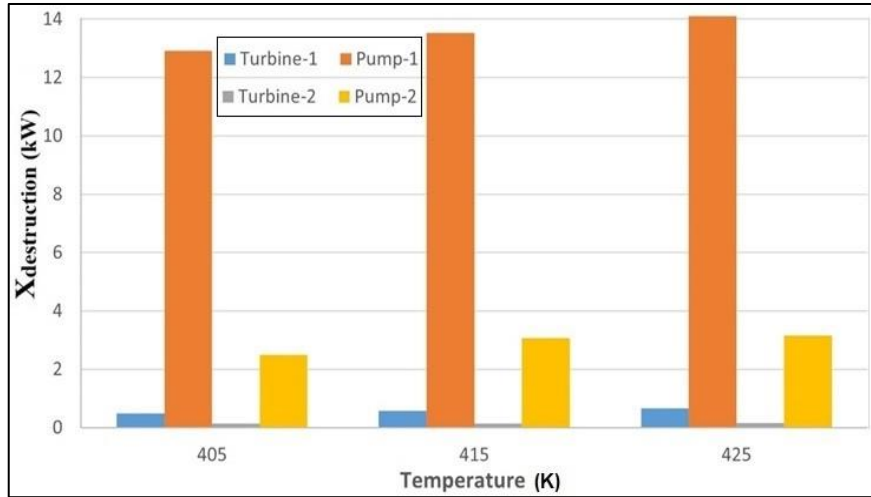


Figure 9. Exergy destruction at turbines and pumps for 405K, 415K and 425K

4. CONCLUSION

This work represents a comprehensive assessment of exergy analysis of the double stage ORC system. The Engineering Equation Solver is used to carry out various calculation of present analysis. In this work, the exergy destruction and exergy efficiency values of various components are obtained and compared.

- The exergy destruction in Pump-1 is found higher than other components at all evaporator inlet temperature. As a result, at 425K, 14.11kW exergy destruction is obtained. The smallest exergy destruction is observed in Turbine-2. The exergy destruction in turbine-2 is found to be 0.133kW at 400K temperature.
- The highest exergy efficiency is observed at the Turbine-2 as 98.48%. The minimum exergy efficiency is seen at the Condenser-1 for 425K temperature as 0.7%.
- The highest thermal and exergy efficiencies of the whole system were obtained at 400K temperature as 8.85% and 48.55%, respectively. The exergy efficiency of the cycle decreases with increase in evaporator inlet temperature. At same time, thermal

efficiency of the system decreases with increase in evaporator inlet temperature.

5. REFERENCES

1. Dincer, I., 6/2000. Renewable Energy and Sustainable Development: A Crucial Review. *Renew Sustain Energy Rev*, 4:157e75.
2. Roy, J.P., Mishra, M.K., Misra, A., 2011. Performance Analysis of an Organic Rankine Cycle with Superheating Under Different Heat Source Temperature Conditions. *Applied Energy*, 88, 2995–3004.
3. Di Pippo R., 2004. Second Law Assessment of Binary Plants Generating Power from Low-temperature Geothermal Fluids. *Geothermics*, 33, 565–86.
4. Wang, D., Ling, X., Peng, H., 2012. Performance Analysis of Double Organic Rankine Cycle for Discontinuous Low Temperature Waste Heat Recovery. *Appl Therm Eng*, 48, 63–71.
5. Tchanche, B.F., Lambrinos, G., Frangoudakis, A., Papadakis, G., 2011. Low-grade Heat Conversion into Power Using Organic Rankine Cycles—A Review of Various Applications. *Renew. Sustain Energy Rev*, 15, 3963–3979.
6. Wang, Q., Wang, J., Li, T., Meng, N., 2020. Techno-economic Performance of Two-stage

Series Evaporation Organic Rankine Cycle with Dual-level Heat Sources. Applied Thermal Engineering, 171, 115078.

7. Bertrand, F.T., Papadakis, G., Lambrinos, G., Frangoudakis, A., 2009. Fluid Selection for a Low Temperature Solar Organic Rankine Cycle. Applied Thermal Engineering 29, 2468-2476.
8. Wall, G., 1998. Exergetics. Exergy Ecology Democracy, Sweden.
9. Rivero, R., Anaya, A., 1997. Exergy Analysis of Industrial Processes: Energy-economy-ecology. Latin American Applied Research, 27, 191-205.
10. Kotas, T.J., 1995. The Exergy Method of Thermal Plant Analysis, Kriger Publishing Comp, USA.
11. Tantekin, A., Tumen Ozdil, N.F., Segmen, M.R., 2015. Thermodynamic Analysis of an Organic Rankine Cycle (ORC) Based on Industrial Data. Applied Thermal Engineering, 91, 43-52.
12. Çengel, A.Y., Boles, M.A., 1998. Thermodynamics, an Engineering Approach, Mc. Graw Hill, USA.
13. Xu, C., Wang, Z., Li, X., Sun, F., 2011. Energy and Exergy Analysis of Solar Power Tower Plants. Appl. Therm. Eng. 31, 3904–3913.
14. Lee, D.H., 2014. Organic Rankine Cycle Power Generator. 8th Fluid Machinery Core Technology Lecture of Korea Society for Fluid Machinery, 169-179.
15. Davidson, T.A., 1977. Design and Analysis of a 1 kW Rankine Power Cycle, Employing a Multi-vane Expander, for Use with a Low Temperature Solar Collector. Master’s Thesis, Massachusetts Institute of Technology, Cambridge, MA, USA.
16. Chen, H., Goswami, D.Y., Stefanakos, E.K., A., 2010. Review of Thermodynamic Cycles and Working Fluids for the Conversion of Low-grade Heat. Renew Sustain Energy Rev, 14, 3059–67.
17. Çengel Y.A., 2003. Heat Transfer. 2th Edition, 690-694.
18. Kaushik, S.C., Reddy, V.S., Tyagi., S.K., 2011. Energy and Exergy Analyses of Thermal Power Plants a Review. Renewable and Sustainable Energy Reviews 15(4), 1857–72.

Nomenclature			
h	Enthalpy [kJkg ⁻¹]		
\dot{m}	mass flow rate [kgs ⁻¹]		
\dot{Q}	heat transfer rate [kW]		
C	heat capacity rate [kW°C ⁻¹]		
T	temperature [°C or K]		
\dot{W}	work [kW]		
A	surface area [m ²]		
<i>Greek Letter</i>			
η	efficiency		
<i>Subscripts</i>			
p	pump	min	minimum
out	outgoing	max	maximum
in	incoming	act	actual
r	re-evaporator	m	mechanic
T	turbine	h	hot
th	thermal	c	cold